Indian Journal of Geo Marine Sciences
Vol. 50 (11), November 2021, pp. 944-953

Numerical investigation of added mass coefficient of a subsea manifold in the accelerating flow and oscillating flow

G Xiang[a,b,c], X B Xiang*[,a,c] & X C Yu[d]

[a]School of Naval Architecture and Ocean Engineering, Huazhong University of Science and Technology, Wuhan – 430 074, China

[b]State Key Laboratory of Fluid Power and Mechatronic Systems, Zhejiang University, Hangzhou – 310 027, China

[c]Hubei Key Laboratory of Naval Architecture and Ocean Engineering Hydrodynamics (HUST), Wuhan – 430 074, China

[d]School of Naval Architecture and Marine Engineering, University of New Orleans, New Orleans, LA, 70148, USA

*[E-mail: xbxiang@hust.edu.cn]

Received 31 August 2021; revised 30 November 2021

The hydrodynamic forces and dynamic responses of subsea equipment, like manifolds, are significantly affected by the motions of the mothership or the unexpected incoming underwater flows like current or internal wave. In this paper, the hydrodynamic coefficients of a simplified subsea manifold, a submerged 3D prism are predicted through the constant acceleration method and forced oscillating method, which are both implemented by the CFD simulation approach. The three directional added mass coefficients of the prism in accelerating flow with different accelerations are obtained. But the value of constant acceleration is found not significantly influencing the added mass coefficient of the rectangular prism. The added mass coefficient of the rectangular prism studied in the paper is 0.233, 0.395, and 2.191 in X, Y and Z direction, respectively. In order to predict the added mass coefficient of the 3D rectangular prism in oscillating flow, the forced oscillating method is used to simulate the rectangular prism oscillating in three directions (X, Y, Z) under different oscillating amplitude and frequency.

[**Keywords**: Added mass coefficient, CFD, Constant acceleration, Forced oscillating, Manifold]

Introduction

The force exerted by a fluid on a bluff body has been of interest to researchers and designers for many years. The complexity of the research has ranged from the simple static case to complicated accelerating cases. When considering an unsteady velocity flow situation, the fluid particles around the object generate an additional inertial force, added mass force. Because of the importance on design of ship, vessels or propulsion devices, etc., the hydrodynamic coefficients such as damping coefficient, added mass coefficient have received wide attention from researchers[1,2].

During the installation of underwater equipment such as manifold from the ocean surface down towards the seabed using crane lifts, manifold will inevitably experience oscillations to cater to the wave excited motion of the installation mothership[3,4] as shown in Figure 1. Also, as shown in Figure 2, the internal horizontal current usually comes up to cause the disruptions of the flow crossing the manifold, greatly influencing the horizontal plane motions of the manifold. The oscillating flow induced by wave and the velocity varying horizontal current will bring significant influence on the hydrodynamic coefficients of the manifold during installations. Correspondingly, the challenges come up which not only regard to the power capabilities and fuel consumptions[5] of the installation mothership but also

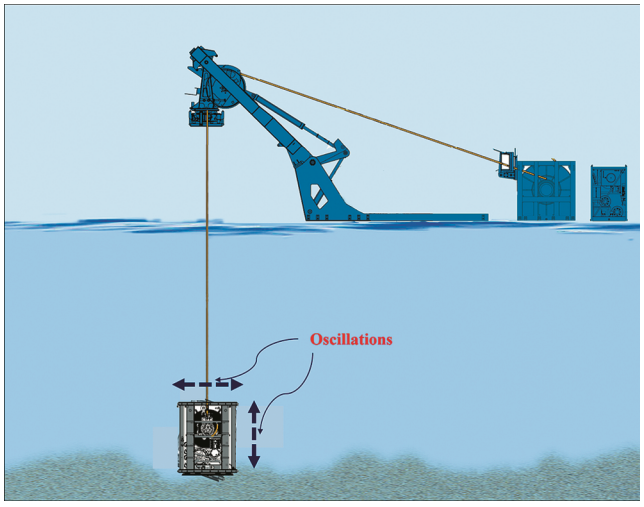

Fig. 1 — Crane lifting operations of the manifold experiencing oscillations induced by the cable

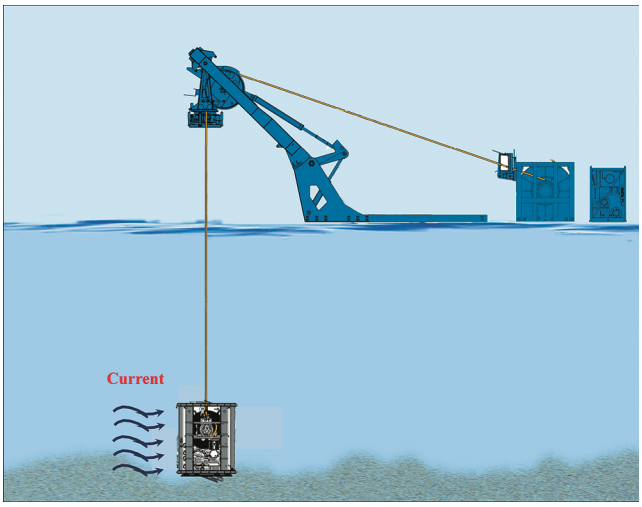

Fig. 2 — Crane lifting operations of the manifold subjecting to the accelerating current

a safe decision making on the installation procedure[6] and efficient motion control analysis of the manifold[7-9]. Finally, the installing operations of manifold will be very complicated problems. Therefore, the most critical part of a lifting installation analysis is to select the correct hydrodynamic coefficients[10].

Currently, there are proper methods to estimate the added mass of an object which are forced oscillation method and constant acceleration method. The forced oscillation method is divided into two branches based on oscillating the body or the flow around the body. To study the effect of sea bottom, many floating or submerged objects are oscillated above sea bottom of different contours or at the different height towards the sea bottom to obtain their hydrodynamic coefficients. Uchiyama[11] applied the finite element method to study the added mass and damping of a circular cylinder oscillating in an air-water bubbly mixture enclosed by a concentric shell. The floor effect has been studied by changing the diameter ratio of the cylinder to the shell. With the diameter ratio increasing, the added mass coefficient increases as well. Zhang & Ishihara[12] presented large-eddy simulations to predict the added mass coefficient of a forced oscillated model with multiple heave plates.

Although the oscillating body method can solve the problem well, it requires too much time cost and very high calculating resources because the mesh around the body needs to be dynamically changed and adapted to the movement of the body at each time step. Thus the oscillating flow method may be a good alternative. Zoontjes[13] compared both methods: oscillating body and oscillating flow method into calculating the added mass and damping coefficients of suction piles using CFD. The authors found that the computational costs for the oscillating flow method are much lower than the oscillating body method. Koo & Kim[14] studied the heave added mass coefficient of various two-dimensional bodies in a finite water depth. At last, simplified formulas are given to predict the heave added mass coefficients at high frequency.

However, the main drawback of the forced oscillation method is that the predicted added mass coefficient may be influenced by the wake induced by the oscillating body because the oscillating body may run into its wake. At this time, constant acceleration method stands out because the wake induced by the translational body is left far behind. Like forced oscillation method, the constant acceleration method can be also divided into two branches: accelerating body[15-18] and accelerating flow[19-21]. The accelerating flow method becomes much more efficient than the accelerating body method because accelerating flow method only needs to solve the static mesh instead of dynamic mesh in accelerating body method. Thus, accelerating flow method deserves more attentions.

In this paper, the constant acceleration method and forced oscillating method are proposed and implemented by CFD approach to predict the hydrodynamic coefficients for a simplified manifold, a 3D rectangular prism. The constant acceleration method based CFD approach is applied to simulate the flow past rectangular prism with different accelerations. The three directional (X, Y, Z) added mass coefficients of the rectangular prism in accelerating flow are obtained for different accelerations. The accelerations are found not significantly influencing the added mass coefficient of the rectangular prism. In order to predict the added mass coefficient of the 3D rectangular prism in oscillating flow, the forced oscillating method based CFD approach is used to simulate the rectangular prism oscillating in three directions (X, Y, Z) under different amplitude and frequency. The effect of the oscillating amplitude and frequency are disclosed via the analysis of the simulation results.

Methodology

This study aims at numerically determining the added mass coefficient of a rectangular prism in the water using both constant acceleration method and forced oscillating method. The open source CFD code, OpenFOAM which has been validated in many

engineering applications[22,23] is now used for numerical simulations.

Constant acceleration method

In this method, a fixed rectangular prism is experiencing an oscillatory incoming flow. According to the Morison equation, the total force acting on the rectangular prism can be expressed as a summation of drag force F_d and inertial force F_I

$$Ft = F_d + F_I \quad \text{... (1)}$$

Where,

$$F_I = \rho\, C_m\, Va \quad \text{... (2)}$$

$$C_m = C_a + 1 \quad \text{... (3)}$$

As a result, by substituting Eq. 2 into Eq. 3, we can get the equation to calculate the added mass coefficient C_a:

$$C_a = \frac{F_I}{\rho Va} - 1 \quad \text{... (4)}$$

Derived from Eq. 1, the inertial force F_I can be obtained by subtracting the drag force from the total force.

$$F_I = Ft - F_d \quad \text{... (5)}$$

Where, ρ: the density of the water; V: the volume of the cylinder; a: the acceleration of the flow; C_a: the added mass coefficient; C_m: inertial coefficient.

During the simulations, we will observe one force jump, which happens at the moment accelerating flow just starts. At this moment, in addition to the drag force, $F_{d,}$ there will be an instantaneous inertial force F_I caused by the accelerations. Also we will observe one force drop that happens at the moment accelerating flow just ends. With the disappearing of the accelerations, the inertial force F_I will also become zero, thus the force drop comes up. Therefore, the critical feature to determine the added mass is the instantaneous change of acceleration that is introduced.

Forced oscillation method

The rectangular prism is vertically forced to oscillate sinusoidally as:

$$X(t) = A \sin(\omega t) \quad \text{... (6)}$$

Where, X(t) is the time-varying displacement in the vertical direction in this study, A is the oscillating amplitude, ω is the oscillating angular frequency ($=2\pi/T$), and T is the oscillating period.

The time series of predicted hydrodynamic force, $F(t)$, is obtained by subtracting the buoyancy force, F_b, from the total predicted force, $F_t(t)$, which is obtained from the surface pressure and shear on the model.

$$F(\mathrm{t}) = F_t(t) - F_b \quad \text{… (7)}$$

Where,

$$F_b = \rho V g \quad \text{…(8)}$$

According to the Morison equation, the hydrodynamic force, $F(t)$, can be expressed as follows:

$$F(\mathrm{t}) = -C_a \rho V \ddot{X}(t) - 0.5 C_d \rho S \left|\dot{X}(t)\right| \dot{X}(t) \quad \text{… (9)}$$

By substituting Eq. 6 into Eq. 9,

$$F(\mathrm{t}) = C_a \rho V A\omega^2 \sin(\omega t) - 0.5 C_d \rho S (A\omega)^2 |\cos(\omega t)| \cos(\omega t) \quad \text{… (10)}$$

Where, S is the characteristic area of the model. As shown in the reference[24], the Fourier averages of C_a can be calculated by:

$$C_a = \frac{1}{\rho V \pi A \omega} \int_0^T F(t) \sin(\omega t)\, \mathrm{d}t \quad \text{… (11)}$$

CFD simulation approach

CFD simulations using constant acceleration method

In constant acceleration method, the rectangular prism with dimensions of $H*L*B$ (H = 0.228 m, L = 1.16 m, B = 0.712 m) is fixed in the domain in Figure 3. The distance of the nearest face of the rectangular prism to the left or right side is $s_1 = 2.5H$, to the top is $s_2 = 4B$, to the bottom is $s_4 = 10B$, to the front or back side is $s_3 = 2.5L$. The top boundary is defined to be inlet for velocity to simulate the downward water flow past the fixed rectangular prism. The velocity at the inlet varies from 0.1 m/s-0.5 m/s but changes with different accelerations of a = 0.02 g and a = 0.04 g, respectively. It is noted that the accelerations during each simulation is a known constant, namely a fixed value. These two predefined time-velocity profiles are expressed as follows:

Profile A:

$$U = \begin{cases} 0.1 & t < 50s \\ 0.1 + 0.02g \times (t - 50) & 50 \le t \le 52s \\ 0.5 & 52 < t < 60s \end{cases}$$

Profile B:

$$U = \begin{cases} 0.1 & t < 50s \\ 0.1 + 0.04g \times (t - 50) & 50 \le t \le 51s \\ 0.5 & 51 < t < 60s \end{cases}$$

The bottom boundary is set to be outlet for pressure. Four vertical sides are defined as solid wall boundaries. The rectangular prism can be rotated to align the side of interest of the rectangular prism with the water flow direction to study the different directional added mass coefficients of the rectangular prism. For example, in Figure 3 is showing the settings for studying transverse coefficient with side *B* aligned with the flow direction. Figure 4 describes the mesh arrangement for studying the added mass coefficients of the rectangular prism in different directions.

CFD simulations using forced oscillating method

The same rectangular prism with dimensions of *H*×*L*×*B* (*H* = 0.228 m, *L* = 1.16 m, *B* = 0.712 m) is oscillated in the computational domain presented in Figure 3 with the predefined motion in Eq. 6. The top boundary for velocity is set to be a mixed condition: pressure-inlet outlet velocity including a zero gradient condition for flow out of the domain and a velocity based on the flux in the patch-normal direction for flow into the domain. A pressure outlet condition was specified: total pressure at the top boundary to set the static pressure from a uniform total pressure. The four vertical sides and the bottom are defined as solid wall boundaries so the velocity at each is set to a fixed value of 0 representing a no-slip and impermeable boundary condition; and the pressure is set to be the zero normal gradient boundary condition. The surface of the rectangular prism is defined as a moving wall with a certain body velocity. The mesh around the rectangular prism will deform with the oscillations of the rectangular prism as shown in Figure 5. Since only the hydrodynamic forces acting on the prism is the focus of research, the SST k-ω turbulence model is selected for modelling the turbulence[25]. But for higher accuracy of simulating flow characteristics

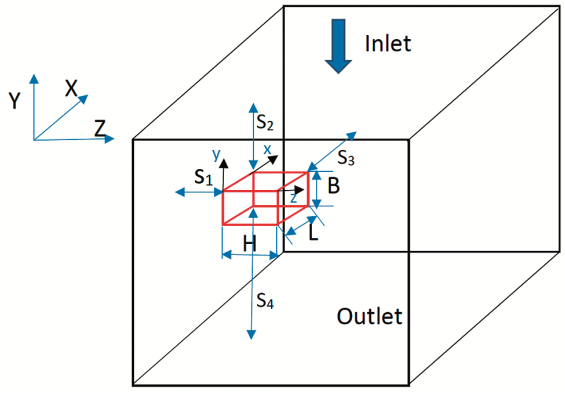

Fig. 3 — Sketch of the downward flow past a fixed 3D rectangular prism

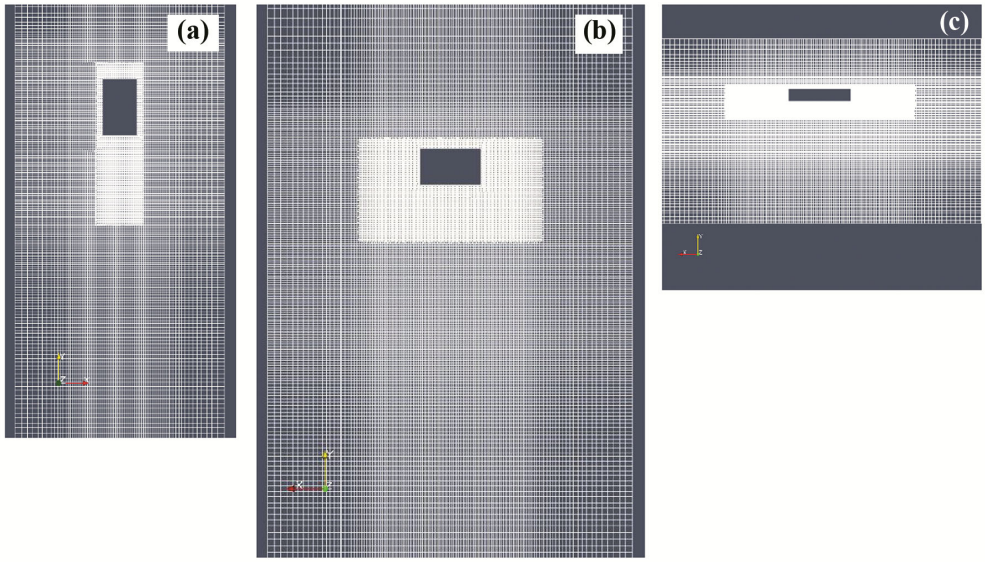

Fig. 4 — Mesh arrangement for studying different directional added mass coefficients of the rectangular prism: (a) longitudinal direction with side *L* aligned, (b) transverse direction with side *B* aligned, and (c) vertical direction with side *H* aligned with the incoming flow direction

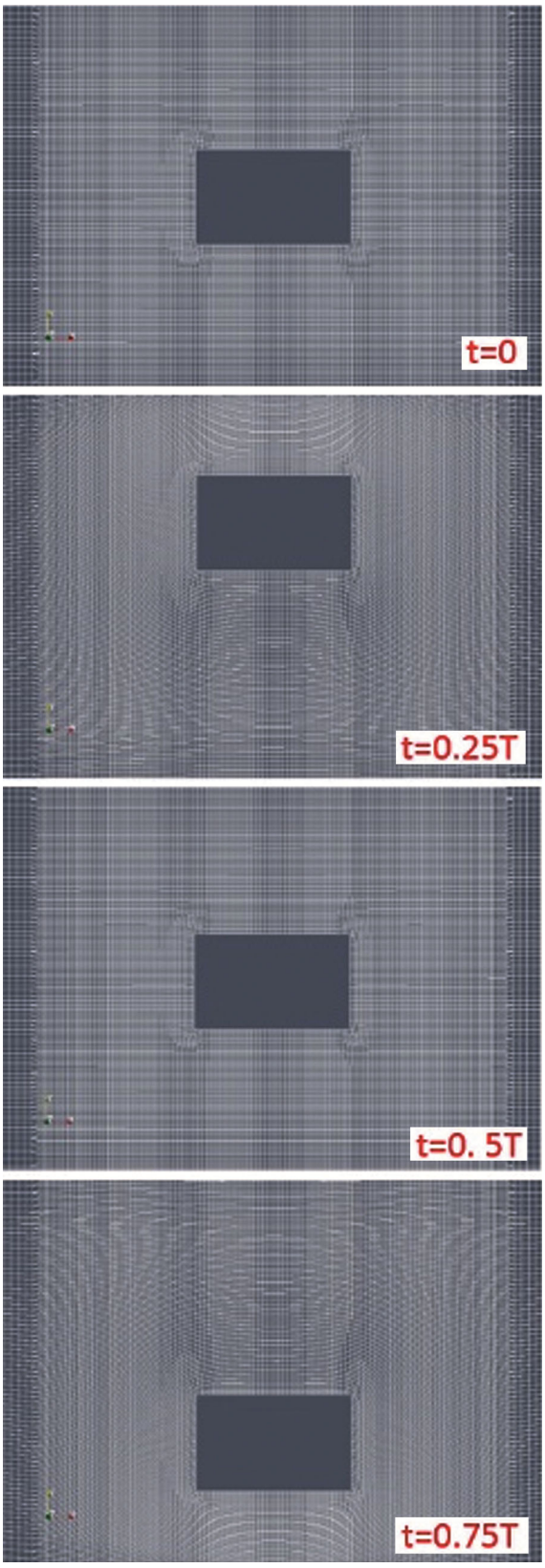

Fig. 5 — Local view of mesh deformations around the rectangular prism in one time period of oscillation

such as flow separations and the large vortex structures behind the prism, Large Eddy Simulations (LES) or Detached Eddy Simulations (DES), are recommended.

Sensitivity study

The sensitivity study mainly focuses on the effect of space resolution and time step on the simulated results.

Table 1 gives information about the sensitivity study on the effect of grid resolution on added mass coefficient of the rectangular prism in transverse direction. Figure 6 shows the effect of grid resolution on the variation of the hydrodynamic force under velocity profile B. By increasing the number of elements, we found that the added mass coefficients become very close.

Table 2 gives information about the sensitivity study on the effect of time resolution on added mass

Table 1 — Added mass coefficient of the rectangular prism at time step of 0.002 s with different grid resolution

Case	Quality	Element	C_a
1	Coarse	80×125×40	0.408
2	Medium	100×150×40	0.403
3	Fine	150×200×50	0.396
4	Finer	200×250×80	0.398

Table 2 — Added mass coefficient of the rectangular prism with Fine mesh at different time step

Case	Time step(s)	C_a
4	0.01	0.409
5	0.005	0.401
6	0.004	0.398
7	0.003	0.396
3	0.002	0.396
8	0.001	0.395

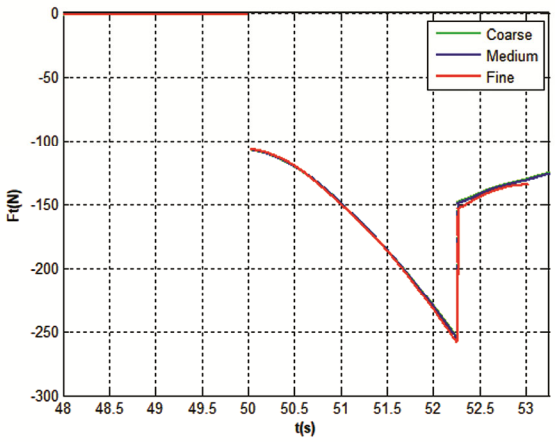

Fig. 6 — Comparison of simulated results due to different space resolutions, variation of total force with time

coefficient in transverse direction. By reducing the time step, we found that the added mass coefficient starts to get converged and become much closer among Case 7 to Case 9, thus, time step of 0.002 s used in Case 6 will be used for the following study.

Validation study

There is neither published experimental data nor related simulation results of the above-mentioned rectangular prism with dimensions of H*L*B (H = 0.228 m, L = 1.16 m, B = 0.712 m). So, in order to validate the CFD simulations into predicting the added mass of an object, a relatively simple model, a 2D cylinder of diameter, d = 0.02 m is selected for the first trial. Table 3 compares the simulated drag coefficients for the 2D cylinder with corresponding experimental data in Horner[26] and Gao[27]. Table 4 presents the simulated added mass coefficients of the 2D cylinder using constant acceleration method of a = 0.01 g, 0.02 g, 0.03 g, and 0.04 g.

Also, the final simulated directional added mass coefficients C_A as expressed by Eq. 12 are obtained by averaging the C_a under different accelerations in Table 4.

$$C_A = \frac{\sum_1^N C_a}{N} \quad \text{... (12)}$$

Where N is the number of simulation cases.

In Table 5, it is found that the simulated drag coefficients match the experimental values very well. The simulated added mass coefficient of the 2D cylinder is 1.02, which is very close to the theoretical value of 1.0.

Results and Discussion

Rectangular prism in accelerating flow

Table 6 shows the simulated added mass coefficients, C_a of a rectangular prism under four velocity profiles with accelerations of 0.02 g, 0.04 g, 0.2 g, and 0.4 g in vertical direction, respectively. It is found that when acceleration increases from 0.02 g to 0.2 g, the C_a in vertical direction increases from 2.19 to 2.325, by about 6 %. The effect of acceleration seems to be very small. Tables 7 & 8 show the simulated added mass coefficients, C_a of a rectangular prism under two velocity profiles with accelerations of 0.02 g, 0.04 g in longitudinal and transverse direction, respectively. The final simulated three directional added mass coefficients C_A are listed in Table 9.

Rectangular prism subjecting to oscillations

In the forced oscillating simulations there are 7 cases to run for each direction as shown in Table 10. Case 1 to Case 5 will study the effect of time period on the predicted added mass coefficient. Case 4, 6 and 7 studies the effect of oscillating amplitude.

Table 3 — Drag coefficients of 2D cylinder

Case	Re	C_d
Horner (1970)	2000	1.0
Gao et al.(2018)	2000	1.05
Present	2000	1.05
Horner (1970)	10000	1.1
Gao et al.(2018)	10000	1.4
Present	10000	1.2

Table 4 — Added mass coefficient of a 2D cylinder under each profile

a	$F_{I1}(N)$	$F_{I2}(N)$	F_I	C_a
0.01g	0.00019	0.000201	0.000195	1.07
0.02g	0.000379	0.000377	0.000378	1.01
0.03g	0.000569	0.000566	0.000567	1.01
0.04g	0.000759	0.000756	0.000757	1.01

Table 5 — Comparison of C_A with theoretical value

Case	C_A
CFD	1.02
Theoretical value	1.00

Table 6 — Vertical added mass coefficient of the rectangular prism under each profile

a	$F_{I1}(N)$	$F_{I2}(N)$	$F_I(N)$	C_a
0.02g	122.058	118.35	120.20	2.190
0.04g	244.48	236.10	240.29	2.192
0.2g	1219.26	1316.68	1267.97	2.325
0.4g	2438.92	2569.95	2504.44	2.367

Table 7 — Longitudinal added mass coefficient of the rectangular prism under each profile

a	$F_{I1}(N)$	$F_{I2}(N)$	$F_I(N)$	C_a
0.02g	46.49	46.38	46.44	0.233
0.04g	93.00	92.80	92.9	0.233

Table 8 — Transverse added mass coefficient of the rectangular prism under each profile

a	$F_{I1}(N)$	$F_{I2}(N)$	$F_I(N)$	C_a
0.02g	52.62	52.43	52.52	0.395
0.04g	105.21	105.08	105.146	0.396

Table 9 — List of the final C_A in different directions

Direction	C_A
Longitudinal	0.233
Transverse	0.395
Vertical	2.191

Table 10 — List of cases simulated in the forced oscillating test

Case	T(s)	A(m)	ω(rad/s)
1	1	0.05	6.283
2	2	0.05	3.141
3	3	0.05	2.094
4	4	0.05	1.570
5	5	0.05	1.256
6	4	0.1	1.570
7	4	0.25	1.570

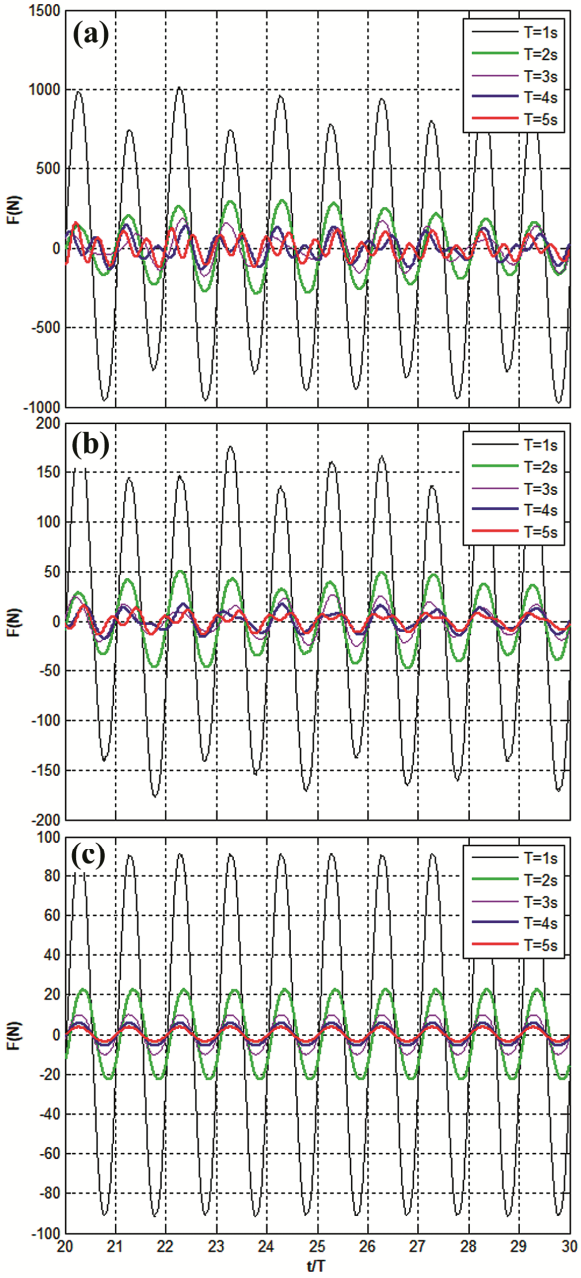

Fig. 7 — Time series of predicted hydrodynamic force acting on the rectangular prism with different time period: (a) vertical, (b) transverse, and (c) longitudinal

Results of hydrodynamic force

The time histories of hydrodynamic force on the rectangular prism are shown in Figures 7 & 8. Figure 7 presents the comparison between different time periods from 1 to 5 s. Figure 8 studies the effect of oscillating amplitude varying from 0.05 to 0.25 m on

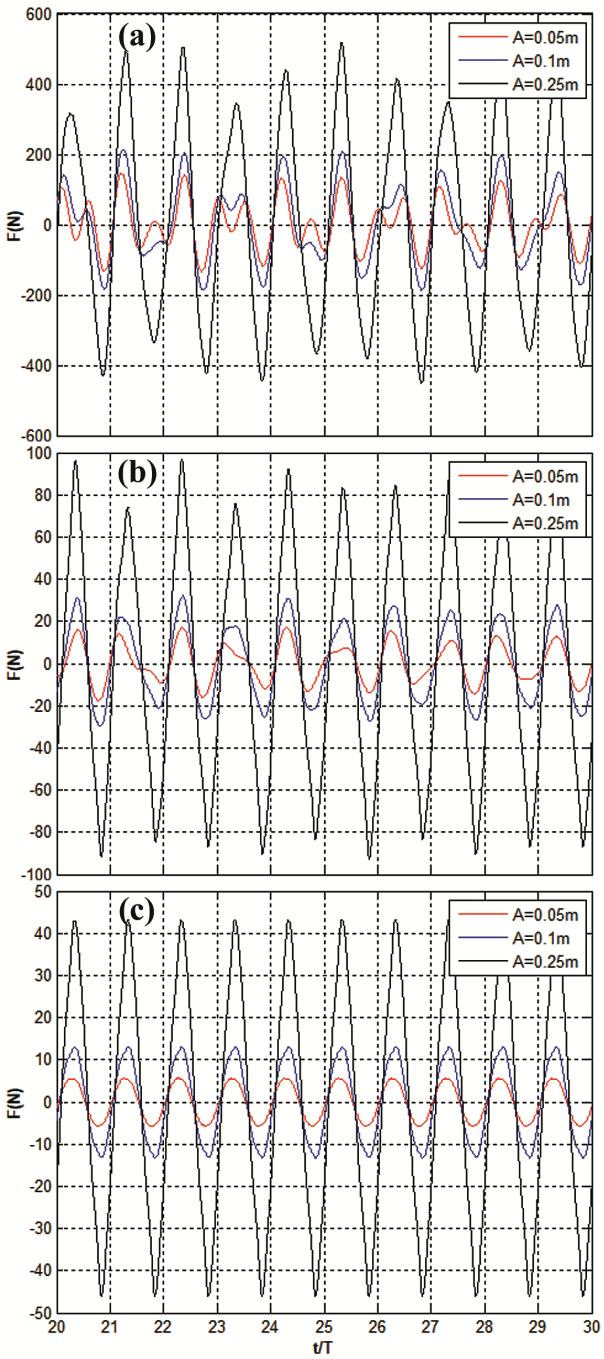

Fig. 8 — Time series of predicted hydrodynamic force acting on the rectangular prism with different oscillating amplitude: (a) vertical, (b) transverse, and (c) longitudinal

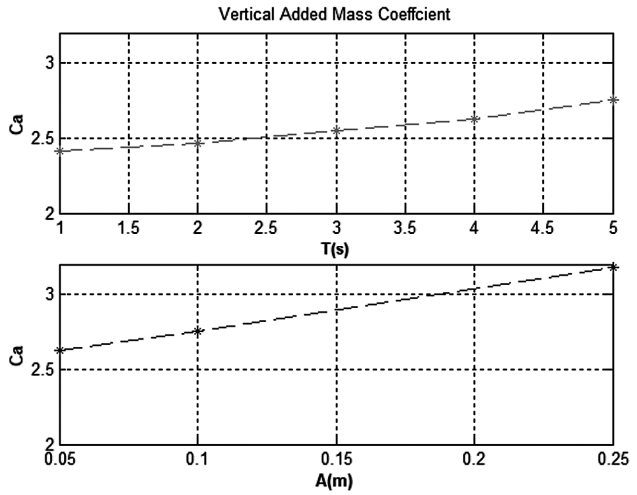

Fig. 9 — Added mass coefficients in vertical direction with different time period (top) and different oscillating amplitude (bottom)

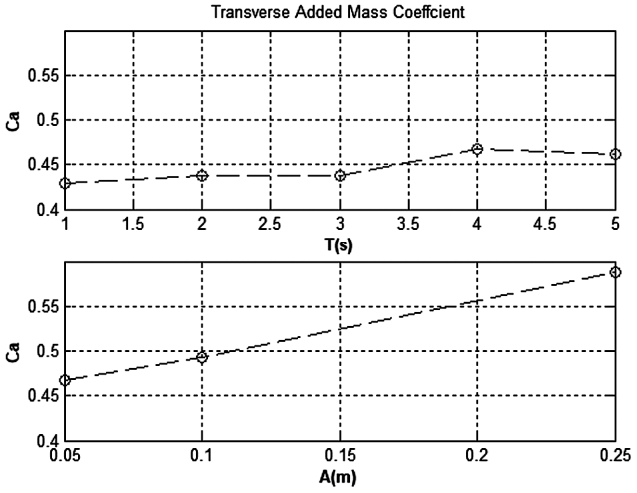

Fig. 10 — Added mass coefficients in transverse direction with different time period (top) and different oscillating amplitude (bottom)

the predicted hydrodynamic forces. It can be observed that under the oscillations, the hydrodynamic force acting on the rectangular prism also starts to oscillate regularly. With the increased oscillating time period, the oscillation amplitude of the hydrodynamic force decreases. This is expected because with larger oscillating period, the moving velocity of the prism will be smaller, which directly gives rise to a smaller drag force. But with the increased oscillating amplitude, the oscillations of the hydrodynamic force curve become significant as well. The explanations are similar. With larger oscillating amplitude, the prism still needs to finish the oscillating cycle within the same time, thus the moving velocity of the prism

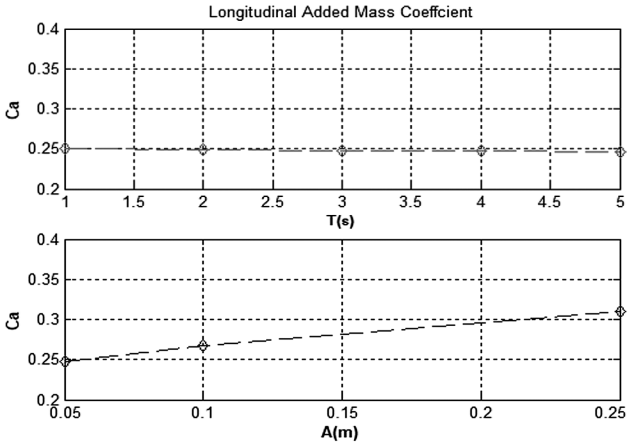

Fig. 11 — Added mass coefficients in longitudinal direction with different time period (top) and different oscillating amplitude (bottom)

will be larger and resultant drag force will increase as well.

Results of added mass coefficient

After obtaining the hydrodynamics forces, the added mass coefficient can be calculated by Eq. 11. Figures 9 – 11 show the added mass coefficient in vertical, transverse and longitudinal directions respectively with different time period and oscillating amplitude. It can be found that the effect of time period on the rectangular prism is large only in vertical direction but are very small in transverse and longitudinal directions. One can see that the *Ca-T* curves are almost flat in transverse and longitudinal directions. However, the effect of oscillating amplitude maintains very large in all the three translational directions. This finding can be obtained by checking the *Ca-A* curve.

Conclusions

In this paper, the constant acceleration method and forced oscillating method based CFD approaches are proposed to predict the added mass coefficients for a 3D rectangular prism in accelerating flow and oscillating flow respectively. The three directional added mass coefficients of the rectangular prism in accelerating flow with different accelerations are obtained. The final added mass coefficient of the rectangular prism studied in the paper is 0.233, 0.395, and 2.191 in X, Y and Z direction, respectively. Then the forced oscillating method is used to simulate the rectangular prism oscillating in three directions under different amplitude and frequency. The effect of the

oscillating amplitude and frequency are disclosed via the analysis of the simulation results.

During the real crane lifting operations, the oscillations of the prism as shown in Figure 1 and the accelerating flow past the prism as shown in Figure 2 will are very likely to exist at the same time. Therefore, in order to make the predictions much closer to the real situations, in the future, the added mass coefficient of oscillating prism in the current should be systematically studied.

Acknowledgements

This work is supported by National Natural Science Foundation of China (under Grant 52071153) and the Open Foundation of the State Key Laboratory of Fluid Power and Mechatronic Systems (under Grant GZKF-202001), in part by the Fundamental Research Funds for the Central Universities (under Grant 2021XJJS016)

Conflict of Interest

There is no conflict of interest.

Author Contributions

GX: Numerical simulation, writing original draft, and data processing; XBX: Resources, Methodology and Writing—review and editing; and XCY: Writing—review and editing.

References

1 Hu L F, Gong Q T, Yuan Z M, Wang X Y & Duan J X, A Roll Damping Analysis of a Standard US Naval Hull Form (DTMB 5415), *Int J Marit Eng*, 163 (2021) 81-89.

2 Kumar A, Vijayakumar R & Subramanian V A, Numerical Fluid-Structure Interaction Analysis for a Flexible Marine Propeller Using Co-Simulation Method, *Int J Marit Eng*, 163 (2021) 79-86.

3 Kang H S, Kim M H & Aramanadka S S B, Numerical Analysis on Mathieu Instability of a Top-Tensioned Riser in a Dry-Tree Semisubmersible, *J Offshore Mech Arct Eng*, 142 (2) (2020) pp. 10. doi.org/10.1115/1.4045094

4 Xiang G & Xiang X B, 3D trajectory optimization of the slender body freely falling through water using Cuckoo Search algorithm, *Ocean Eng*, 235 (2021) p. 109354.

5 Chiong M-C, Kang H-S, Shaharuddin N M R, Mat S, Quen L K, *et al*., Challenges and opportunities of marine propulsion with liquid alternative fuels, *Renew Sust Energ Rev*, 149 (2021) p. 111397. doi.org/10.1016/j.rser.2021.111397

6 Xiang X B, Yu C Y & Zhang Q, On intelligent risk analysis and critical decision of underwater robotic vehicles, *Ocean Eng*, 140 (2017) 453-465.

7 Zhang Q, Zhang J L, Chemori A & Xiang X B, Virtual Submerged Floating Operational System for Robotic Manipulation, *Complexity*, (2018) 1–18. doi: 10.1155/2018/9528313

8 Kang H S, Kim M H, Aramanadka S S B & Kang H Y, Semi-Active Magneto-Rheological Damper to Reduce the Dynamic Response of Top-Tension Risers, In: *Proceedings, 23rd Int Offshore and Polar Engineering Conf*, June 30 - July 5, 2013, Anchorage, Alaska, USA.

9 Wang Z, Yang S L, Xiang X B, Vasilijevic A, Mišković N, *et al.*, Cloud-based mission control of USV fleet: architecture, implementation and experiments, *Control Eng Pract*, 106 (2021) p. 104657.

10 Xiang G & Soares G C, Improved Dynamic Modelling of Freely Falling Underwater Cylinder Based on CFD, *Ocean Eng*, 211 (2020) p. 107538.

11 Uchiyama T, Numerical prediction of added mass and damping for a cylinder oscillating in confined incompressible gas–liquid two-phase mixture, *Nucl Eng Des*, 222 (2003) 68-78.

12 Zhang S N & Ishihara T, Numerical study of hydrodynamic coefficients of multiple heave plates by large eddy simulations with volume of fluid method, *Ocean Eng*, 163 (2018) 583-598.

13 Zoontjes R, Siegersma H & Ottens H, Using CFD to Determine Heave Added Mass and Damping of a Suction Pile, In: *Proceedings of the ASME 2009 28th International Conference on Ocean, Offshore and Arctic Engineering OMAE2009*, May 31 - June 5, 2009, Honolulu, Hawaii, USA.

14 Koo W & Kim J, Simplified formulas of heave added mass coefficients at high frequency for various two-dimensional bodies in a finite water depth, *Int J Nav Archit Ocean Eng*, 7 (2015) 115-127.

15 Fernandes A C & Mineiro F P S, Assessment of hydrodynamic properties of bodies with complex shapes, *Appl Ocean Res*, 29 (2007) 155-166.

16 Hu X Z & Liu S J, Simulation and calculation of hydrodynamic forces of components of deep sea mining system, *2010 International Conference on Digital Manufacturing & Automation*, December 18 - 20, 2010, Changsha, China.

17 Raza N, Mehmood I, Rafiuddin H & Rafique M, Numerical simulation of added mass determination of standard ellipsoids, *Proceedings of 2012 9th International Bhurban Conference on Applied Sciences & Technology (IBCAST)*, 9 – 12 Jan. 2012, Islamabad, Pakistan.

18 Yang J, Feng J F, Li Y L, Liu A, Hu J H, *et al*., Water-Exit Process Modeling and Added-Mass Calculation of the Submarine-Launched Missile, *Pol Marit Res*, 95 (2017) 152-164.

19 Mishra V & Bhattacharya S, Translational Added Mass of Axisymmetric Underwater Vehicles with Forward Speed Using Computational Fluid Dynamics, *J Sh Res*, 55 (3) (2011) 185–195.

20 Javanmard E, Mansoorzadeh S & Mehr J A, A new CFD method for determination of translational added mass coefficients of an underwater vehicle, *Ocean Eng*, 215 (2020) p. 107857.

21 Xiang G & Soares G C, A CFD Approach for Numerical Assessment of Hydrodynamic Coefficients of an Inclined Prism near the Sea Bottom, *Ocean Eng*, 2021, Under review.

22 Yang J M, Tian X L & Li X, Hydrodynamic characteristics of an oscillating circular disk under steady in-plane current conditions, *Ocean Eng*, 75 (2014) 53-63.

23 Xiang G, Wang S & Soares G C, Study on The Motion of a Freely Falling Horizontal Cylinders into Water Using OpenFOAM, *Ocean Eng*, 196 (2020) p. 106811.
24 Sarpkaya T, Wave Forces on Offshore Structures, *Cambridge University Press*, 2010.
25 Menter F R, Kuntz M & Langtry R, Ten years of industrial experience with the SST turbulence model, In: *Proceedings of the fourth international symposium on turbulence, heat and mass transfer*, Antalya, Turkey, Begell House, 2003, pp. 625–632.
26 Hoerner S, Fluid Dynamic Drag: Practical Information on Aerodynamic Drag and Hydrodynamic Resistance, 2nd Edn, (Hoerner Fluid Dynamics, Bakersfield, Calif), 1965, pp. 460.
27 Gao W, Nelias D & Liu Z, Numerical investigation of flow around one finite circular cylinder with two free ends, *Ocean Eng*, 156 (2018) 373-380.